Agricultural Water Management 203 (2018) 366–375

Contents lists available at ScienceDirect

Agricultural Water Management

journal homepage: www.elsevier.com/locate/agwat

# Comparison of three crop water stress index models with sap flow measurements in maize

Ming Han[1], Huihui Zhang*, Kendall C. DeJonge, Louise H. Comas, Sean Gleason

*Water Management and Systems Research Unit, USDA-ARS, 2150 Centre Avenue, Bldg. D., Suite 320, Fort Collins, CO 80526, United States*

ARTICLE INFO

*Keywords:*
Empirical CWSI
Theoretical CWSI
Aerodynamic resistance
Water stress
Deficit irrigation

ABSTRACT

Both empirical and theoretical models have been widely used to calculate a crop water stress index (CWSI) − a metric often used to describe crop water status. The purpose of this study was to determine the accuracy, limitation, and uncertainty of an empirical (CWSI-E) and two theoretical models compared with sap flow measurement in maize. One theoretical model used a calculated aerodynamic resistance (CWSI-T1), and the other theoretical model used seasonal average aerodynamic resistance (CWSI-T2). Considering the uncertainty of crop coefficient and sap flow measurement, CWSI-T2 and CWSI-E models gave reasonable overall estimates of water stress. The average root mean square deviation at each growth stage from each model ranged from 0.16 to 0.33. CWSI-T2 and the CWSI-E provided relatively accurate prediction of crop stress, both between growth stages and irrigation events. However, CWSI-T1 did not accurately predict water stress between growth stages or between irrigation events. By including climate factors, crop water stress estimated by CWSI-T2 showed less variation and uncertainty than CWSI-E. The uncertainty of both CWSI-T2 and CWSI-E decreased with increasing vapor pressure deficit (VPD), and CWSI-E show larger crop water stress prediction uncertainty. The intercept of non-water stress baseline was the main source of the uncertainty for CWSI-E and CWSI-T2. Considering both uncertainty and stability, we recommend CWSI-T2 model (i.e., seasonal average aerodynamic resistance) for maize water stress assessment.

## 1. Introduction

Agriculture is a major water user in semi-arid regions, and utilizing agricultural water efficiently is critical to sustain and maximize the benefits of limited irrigation water. Water resources for agriculture have been reduced due to drought associated with climate change, non-sustainable use of groundwater, and increased competition from municipal, environmental, and industrial water needs. Combined with the increasing global population, there is a need to achieve maximum production per unit of applied irrigation water. Regulated deficit irrigation, defined as a regime that purposely reduce applied irrigation water in specific crop growing stages (Chalmers et al., 1981), may be a way to achieve higher water productivity (i.e., crop produced per unit water consumed). However, a comprehensive knowledge of crop response and crop water use under water stress is needed to achieve the best balance between irrigation water use and crop yield (Geerts and Raes, 2009). Therefore, the development of tools that enable accurate estimation of crop water stress or crop water use is critical for deficit irrigation management.

The crop water stress index (CWSI) has been recognized as an indicator of plant water status based on canopy temperature, ambient air temperature, and relative humidity. Two methods for calculating CWSI have been widely used and evaluated: an empirical method (CWSI-E) developed by Idso et al. (1981) and a theoretical method (CWSI-T1) developed by Jackson et al. (1981). The empirical method establishes a relationship between canopy-to-air temperature difference and vapor pressure deficit (VPD). The theoretical method uses surface energy balance equation, whilst accounting for variation in climate, and calculates the divergence between the upper and lower boundaries of canopy-to-air temperature difference. CWSI calculated from both methods have shown good relationships with other crop water stress indicators, such as soil water content (DeJonge et al., 2015; Taghvaeian et al., 2012; Taghvaeian et al., 2014a; Wang et al., 2005) and leaf water potential (Ballester et al., 2013; Gonzalez-Dugo et al., 2014). CWSI from both methods have also been used for irrigation scheduling (Colaizzi et al., 2012; Emekli et al., 2007; Nielsen, 1990; O'Shaughnessy et al., 2010; Yazar et al., 1999).

However, there remain limitations of both methods that require

* Corresponding author.
*E-mail address:* Huihui.Zhang@ars.usda.gov (H. Zhang).

[1] Current affiliation: Department of Civil and Environmental Engineering, University of Waterloo, Waterloo, ON, Canada.

https://doi.org/10.1016/j.agwat.2018.02.030
Received 1 November 2017; Received in revised form 23 February 2018; Accepted 24 February 2018
0378-3774/ Published by Elsevier B.V.

careful consideration. The empirical method has been criticized for two reasons: 1) sensitivity of the empirical non-water stress baseline to the changes of climate variables, such as radiation and wind speed (Gonzalez-Dugo et al., 2014; Jackson et al., 1988; Payero and Irmak, 2006). For example, the empirical baseline may change yearly for the same crop in the same field. Horst et al. (1989) has reported significant differences ($P < 0.01$) between the CWSI baseline equations in 1986 and 1987 for common Bermuda grass, buffalo grass and tall fescue. A similar result has been reported for mandarin and orange (Gonzalez-Dugo et al., 2014). 2) CWSI calculated by the empirical method showed large fluctuations, especially under low VPD condition or with significant variation in climate (Stockle and Dugas, 1992). Compared to the empirical method, the advantage of CWSI-T1 is its stability under various climate conditions (Jackson et al., 1988; Yuan et al., 2004). The shortcoming of CWSI-T1 is that it may not give significantly different values for well-watered and stressed crops, which may attribute to the incorrect estimation of aerodynamic resistance, $r_a$ (Agam et al., 2013; Stockle and Dugas, 1992). Jackson et al. (1988) suggested that a seasonal average aerodynamic resistance should be applied (CWSI-T2). There are several successful applications of theoretical approach by calculating a seasonal average aerodynamic resistance (Clawson et al., 1989; Jalali-Farahani et al., 1993).

Therefore, it is important to know the accuracy and consistency of these three models for CWSI calculation before any application. As mentioned previously, many studies have proven good relationships between CWSI and measured water stress indicators; however, few had used sap flow measurement to assess the accuracy and consistency of CWSI models. Sap flow methodology, which provides a measurement of whole plant transpiration, has been widely used to determine crop coefficient and evaluate simulated crop water transpiration and crop water stress by various models (Cammalleri et al., 2013; Chabot et al., 2002; Jara and Stockle, 1999; Zhao et al., 2015). The transpiration measurement by sap flow would have 5% to 10% of actual transpiration error, which have been obtained by comparing with other measurements (Green et al., 2003; Zhang et al., 2011). The performance of CWSI models can be evaluated by comparing model outputs with water stress determined from sap flow measurement.

The objectives of this study were to: 1) compare the performance of CWSI among one empirical model and two theoretical models with sap flow measurement; 2) evaluate the uncertainty among the three CWSI models.

## 2. Materials and methods

### 2.1. Field experiment

#### 2.1.1. Study site and management

Field data were collected from maize during the 2015 growing season at USDA-ARS Limited Irrigation Research Farm (LIRF), in Greeley, Colorado, USA (40°26′57″N, 104°38′12″W, elevation 1427 m). The alluvial soils of the study field were predominantly sandy and fine sandy loam of Olney and Otero series. The maize (Zea mays L.) was planted on Jun 1, 2015 with planting density around 85,000 plants $ha^{-1}$, and the dates when maize reached the late vegetative stage (V8), beginning of reproductive stage (R1), beginning of maturation stage (R3), and harvest were Jul 9, Aug 2, Aug 24 and Nov 2, 2015, respectively. Final plant populations varied from 77,000 to 82,000 plants $ha^{-1}$. Deficit irrigation was regulated by withholding during the late vegetative growth stage (V8 to R1) and/or the maturation growth stage (R3 to R6), but applying water during the sensitive reproductive (R1 to R3) and early vegetative stages (planting to V8). A total of 12 irrigation treatments were arranged in a randomized block design consisting of four blocks with each treatment replicated once in each block. Each treatment plot had 12 rows at 0.76 m spacing (9 m wide by 43 m long). All measurements were taken from the middle four rows to reduce border effects. Treatments are named for the target percent of maximum non-stressed crop ET (Evapotranspiration) during late vegetative and maturation growth stages, respectively (e.g. a 40/80 treatment would target 40% of maximum ET during the vegetative stage and 80% of maximum ET during the maturation stages). Sap flow measurements were taken in 100/100, 65/65, 40/40, and 40/80 treatments, so only these four treatments were included in this study and the actual irrigation amounts that were achieved for the four treatments are shown in Table 1. During the growing season, irrigation water was applied through a surface drip irrigation system with drip tubing (16 mm outside diameter, 2 mm wall thickness, 30 cm in-line emitter spacing, 1.1 L $h^{-1}$ emitter flow rate) placed on the soil surface next to each row of maize. Irrigation applications to each treatment were measured with turbine flow meters (Badger Recordall Turbo 160 with RTR transmitters). Meters were cross calibrated to ensure accuracy and consistency. Irrigation applications were controlled by and recorded with a Campbell Scientific CR1000 data logger. A constant pressure water supply controlled with a variable speed drive booster pump, low pressure loss in the delivery system, and relatively flat topography resulted in predicted water distribution uniformity among and within plots exceeding 95% (Trout and Bausch, 2017). Nitrogen fertilizer (Urea ammonium nitrate, UAN, 32%) was applied near the seed at planting at 34 kg N $ha^{-1}$. Additional nitrogen was applied through the irrigation water (fertigation) to meet fertility requirements in all the treatments. More details for calculation of maximum ET and measurement of soil water deficit can be found in DeJonge et al. (2015).

Hourly meteorological data were acquired by an on-site standard ET weather station (10 m away from the field), which is belong to Colorado Agricultural Meteorological Network (CoAgMet, http://ccc.atmos.colostate.edu/~coagmet/). The data includes precipitation, air temperature, relative humidity (and subsequent vapor pressure deficit), solar radiation, and wind speed taken at 2 m above a grass reference surface. The net solar radiation was determined following the procedure in Allen et al. (1998) and Jensen and Allen (2016). The crop phenology developments as well as basic climate factors in each stage were shown in Table 2.

**Table 1**
Irrigation treatments evaluated in the study, with irrigation and precipitation amounts (mm) during major growth stages in 2015. The values on either side of the '/' denote the target ET values for vegetative and maturation stages of development. For example, 40/80 indicates that 40% of maximal ET was applied during vegetative growth stage and 80% of maximal ET was applied during maturation growth stage.

| Treatment (% vegetative ET/% maturation ET) | Vegetative | Reproductive | Maturation |
|---|---|---|---|
| | Jun 2–Aug 1 | Aug 2–Aug 24 | Aug 25–Nov 3 |
| 100/100 | 166 | 116 | 200 |
| 65/65 | 84 | 112 | 70 |
| 40/40 | 40 | 113 | 0 |
| 40/80 | 40 | 111 | 149 |
| Precipitation | 76 | 23 | 38 |

#### 2.1.2. Canopy ground cover, yield and temperature measurements

A Canon EOS 50D DSLR camera (Canon Inc., Tokyo, Japan)[2] was used to measure canopy ground cover. The camera was attached to a boom that was mounted on a high clearance tractor so that the camera was elevated about 7 m above the ground. Nadir view RGB images were taken near solar noon twice a week from each treatment plot. The camera field of view encompassed 4 rows × 4 m. All images were processed in Python 3.5 (Python Software Foundation, Wilmington, DE,

[2] Mention of trade names or commercial products in this publication is solely for the purpose of providing specific information and does not imply recommendation or endorsement by the U.S. Department of Agriculture.

**Table 2**
Average daily weather conditions during the growing season (from seeding to harvest) in each crop growth stage. *DAP* is the day after planting and the number in the brackets is the minimum and maximum observations for each variable in the corresponding period; $T_{mean}$ is the mean daily temperature (°C); $R_s$ is the average daily solar radiation (MJ $m^{-2}$); The Sum of the seasonal precipitation was shown in Table 1; $u_2$ is the daily averaged wind speed from 2 m height (km $day^{-1}$); *VP* is the actual vapor pressure (kPa).

| Stage | Vegetative | Reproductive | Maturation |
|---|---|---|---|
| | Jun 2–Aug 1 | Aug 2–Aug 24 | Aug 25–Nov 3 |
| *DAP* | 62 | 82 | 153 |
| $T_{mean}$ (°C) | 21(15, 36) | 21.4(15, 37) | 15.4 (7, 35) |
| $R_s$ (MJ $m^{-2}$) | 22.9(10, 31) | 25(12, 28) | 16.2 (1.5, 24) |
| $u_2$ (m $s^{-1}$) | 2 (0.8, 4) | 1.6 (0.4, 2.7) | 1.2 (0.5, 4.4) |
| *VP* (k Pa) | 1.5 (1.7, 3.29) | 1.4 (1.7, 3.4) | 1.4 (1.0, 3) |

USA) to separate green plant canopy from background (soil, surface residue, and senesced leaves). The canopy ground cover for each treatment during the crop growing season is shown in Fig. 1.

Grain yield was measured by hand harvesting the ears from the center sampling area of the center four rows of each plot. The sampling area was about 69 $m^2$. Grain was threshed with a stationary thresher (Wintersteiger Classic ST, Wintersteiger AG, Ried, Austria), weighed and subsampled for moisture content determination. Grain moisture content at harvest was measured with a DICKEY-john GAC500-XT Moisture Tester (DICKEY-john Corp, Aubern, Ill, USA).

Infrared thermal radiometers (IRT, model: SI-121, Apogee Instruments, Inc., Logan, Utah, USA) were used to monitor continuous canopy temperature of maize. The view angle of IRT was 36° field of view, with ± 0.2 °C accuracy over the temperature range of −10 to 65 °C. The IRTs were attached to telescoping posts and angled 23° below horizon and 45° from north (looking northeast) to ensure the field of view included primarily crop canopy. The viewing area of the IRTs was about 13.35 $m^2$. The IRTs were kept at a height of 0.8 m above the top of canopy throughout the growing season (adjusted twice per week during vegetative growth). An IRT sensor was installed for each plot on Jul 13, 2015, and a total of four IRTs for each treatment. IRT measurements in 100/100, 65/65, 40/40, and 40/80 treatments from Jul 25 to Sept 05, 2015 were used to determine crop water stress. During this period, crop coverage measured from nadir view in all treatments were larger than 0.35 (Fig. 1), and the crop coverage in the field view of IRTs was larger than 0.8. All IRT measurements were recorded by dataloggers (model: CR1000, Campbell Scientific Inc., Logan, Utah, USA), every 5 s and averaged on hourly intervals. Measured values were corrected for the effect of sensor body temperature using calibration equations provided by the manufacturer.

### 2.1.3. Sap flow measurement

Whole plant transpiration was measured on two plants per plot in 100/100, 65/65, 40/40, and 40/80 treatments with stem heat balance sap flow EXO sensors (Dynamax, Inc, Houston, TX, USA) (Sakuratani, 1981), thus a total of eight sensors was installed for each treatment. Accuracy of these sensors was verified in 2015 in a greenhouse study with maize in 15L pots placed on logging scales (van Bavel M, Young J, and Comas L, 2017, Application Report, www.dynamax.com). Data were collected from Jul 28 to Sept 20, 2015. SapIP data loggers (Dynamax, Inc, Houston, TX, USA) were placed approximately 12 m from the end of the plot and sensors were installed on plants randomly chosen in the same row within 3 m from the loggers (Dynamax, Inc, Houston, TX, USA). The bottom 2–3 leaves and leaf sheaths were removed at least a day prior to installing gages. Sensors were then installed on stem internodes that were covered with plastic wrap to prevent moisture from stems from entering the sensors. A thin film of silicon was applied to facilitate thermal exchange between the stems and sensors. Sensors were wrapped from the inside to the exterior with stretchable and wicking Velcro, waterproof fabric sealed with electrical tape at the top, insulating foam, and insulated foil bubble wrap secured with zip ties and sealed with electrical tape at the top. The voltage was set to 4.2–4.3 V dc and resulted in power ranging from 0.20 to 0.27 W depending on the size of sensor. The temperature applied ranged from 0.5 to 4 °C above ambient and there was no stem damage from heat. Data were monitored for abnormalities during measurements, and stems inspected carefully for aberrations upon removal of the sensors. The average value of the thermopile radial heat loss factor (*Ksh*) is established when there is low to zero flow and is required to solve the energy balance of the system. Average *Ksh* was computed during 3:30–5:30 h MST (Mountain Standard Time) and set to the daily *Ksh* at 5:30 h. Since the formula for calculating *Ksh* depends on zero sap flow heat flux, there may be a small error in sap flow calculations if there is transpiration during the period used for *Ksh* computation. We estimate that maximum transpiration loss during this period may be 4 g/hr based on the greenhouse study of fully-watered maize grown in 15L pots that were placed on logging scales and sealed from the top of the pot to the plant stem with plastic garbage (data not shown). If total weight loss from the pots during this period was from transpiration rather than evaporation, total error from the *Ksh* was about 1.6% and not substantial for this application. Sensor outputs were collected every 1 min and recorded as 15-min means from the end of July through September. Sap flow was determined as the mass of water transpired by the plant per unit time (g $h^{-1}$ $plant^{-1}$) and expressed per ground area by dividing by the planting density.

## 2.2. Crop water stress index (CWSI)

CWSI is defined in Eq. (1) by the upper $(T_c - T_a)_u$ and lower

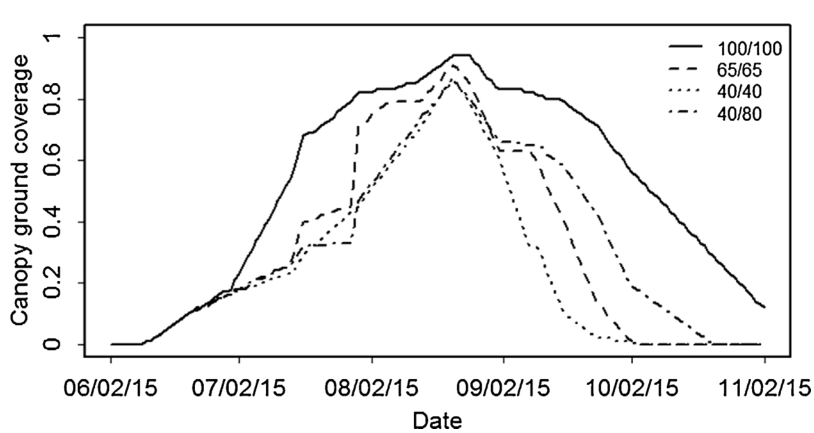


**Fig. 1.** Maize canopy ground cover through the growing season in 2015.

boundary $(T_c - T_a)_l$ of temperature difference between air and canopy, where $(T_c - T_a)_u$ and $(T_c - T_a)_l$ representing a non-transpiring and full transpiring conditions, respectively (Idso et al., 1981; Jackson et al., 1981).

$$CWSI = \frac{(T_c - T_a)_c - (T_c - T_a)_l}{(T_c - T_a)_u - (T_c - T_a)_l} \tag{1}$$

where: $(T_c - T_a)_c$ is the difference between canopy temperature ($T_c$, °C) and air temperature ($T_a$, °C) for the current condition. When the crop is fully watered, CWSI value is close to 0; whereas for the crop under severe water stress condition, CWSI value is close to 1.

The difference between the following CWSI models is the procedure to determine the upper $(T_c - T_a)_u$ and lower $(T_c - T_a)_l$ boundaries.

#### 2.2.1. Empirical model (CWSI-E)

According to Idso et al. (1981), the lower and upper boundary of $(T_c - T_a)$ for various crops under various climatic conditions could be defined as:

$$(T_c - T_a)_l = a - b \times VPD \tag{2}$$

$$(T_c - T_a)_u = a - b \times VPG \tag{3}$$

where: $VPD$ is the vapor pressure deficit of the atmosphere (assuming leaf temperature = air temperature), intercept $a$ and slope $b$ are the linear regression parameters of $(T_c - T_a)_l$ on $VPD$, $VPG$ is the difference between the saturation vapor pressure evaluated at air temperature ($T_a$) and at a higher air temperature equal to air temperature plus "$a$" in Eq. (2) $(T_a + a)$.

#### 2.2.2. Theoretical model 1 (CWSI-T1)

The theoretical development of CWSI is based on surface energy balance equation, which includes the following assumptions: 1) aerodynamic resistance ($r_a$) adequately represents the resistance to turbulent transport of heat, water vapor, and momentum (Jackson et al., 1981; Jackson et al., 1988). Then the temperature difference between canopy and air could be defined as:

$$T_c - T_a = \frac{r_a}{\rho c_p}\frac{\gamma(1 + r_c/r_a)}{\Delta + \gamma(1 + r_c/r_a)}(R_n - G) - \frac{e^* - e}{\Delta + \gamma(1 + r_c/r_a)} \tag{4}$$

where: $c_p$ is the heat capacity of air (J kg$^{-1}$ °C), $T_c$ is the temperature of canopy, $T_a$ is the air temperature, $e^*$ is the air saturated vapor pressure at $T_c$ (Pa), $e$ is the air vapor pressure (Pa), $\gamma$ is the psychrometric constant (Pa °C$^{-1}$), $r_a$ is the aerodynamic resistance (s m$^{-1}$), $r_c$ is the canopy resistance (s m$^{-1}$), $\Delta$ is the change (slope) of saturation vapor pressure with temperature (Pa °C$^{-1}$), $R_n$ is the net radiation (J m$^{-2}$ s$^{-1}$), $G$ is heat flux consumed by soil (J m$^{-2}$ s$^{-1}$), and was assumed around 10% of $R_n$.

Then the upper boundary of $(T_c\text{-}T_a)$ is calculated, when $r_c \to \infty$:

$$(T_c - T_a)_u = \frac{r_a}{\rho c_p}(R_n - G) \tag{5}$$

And the lower boundary of $(T_c\text{-}T_a)$ is calculated, when $r_c = r_{cp}$

$$(T_c - T_a)_l = \frac{r_a}{\rho c_p}\frac{\gamma(1 + r_{cp}/r_a)}{\Delta + \gamma(1 + r_{cp}/r_a)}(R_n - G) - \frac{e^* - e}{\Delta + \gamma(1 + r_{cp}/r_a)} \tag{6}$$

where: $r_{cp}$ is the canopy resistance under full transpiration condition.

According to Jackson et al. (1981); Jackson et al. (1988), $r_{cp}$ was defined as 0 for non-water stress condition. And $r_a$ is calculated by:

$$r_a = \frac{4.72[Ln(z - d)/z_0]^2}{1 + 0.54u} \tag{7}$$

where: $z$ is the reference height (m), $d$ is the displacement height (m), $d = 0.63\,h$, $h$ is the height of crop, $z_o$ is the roughness length (m), $z_o = 0.13\,h$, and $u$ is the wind speed at height $z$ (m s$^{-1}$).

#### 2.2.3. Theoretical model 2 (CWSI-T2)

Several studies have found that the theoretical approach performed well when given a mean $r_a$ and $r_{cp}$ during the study period (Clawson et al., 1989; Jalali-Farahani et al., 1993). Jackson et al. (1988) suggested that seasonal average $\bar{r}_a$ and $r_{cp}$ were reasonable. Thus we calculated the upper and lower boundary of $(T_c - T_a)$ using seasonal average $\bar{r}_a$ and $r_{cp}$, instead of using Eq. (7) for $r_a$ and 0 for $r_{cp}$ in CWSI-T1 approach. They were estimated by (O'Toole and Real, 1986):

$$\bar{r}_a = \frac{\rho c_p a}{\bar{R}_n b(\bar{\Delta} + 1/b)} \tag{8}$$

$$\bar{r}_{cp} = -\bar{r}_a\left(\frac{\bar{\Delta} + 1/b}{\gamma} + 1\right) \tag{9}$$

where: $\bar{R}_n$ is the seasonal average net radiation, $\bar{\Delta}$ is the seasonal average slope of saturated vapor pressure-temperature relationship (Pa °C$^{-1}$), which is determined by seasonal average temperature, $a$ and $b$ are parameters from Eq. (2). The $\bar{r}_a$ and $\bar{r}_{cp}$ were calculated based on non-water stress condition. The $\bar{r}_{cp}$ was only used in non-water stress condition in Eq. (6). Since $r_a$ was not influenced by crop water stress, the $\bar{r}_a$ determined was used in both Eqs. (5)–(6).

### 2.3. Water stress calculation

#### 2.3.1. CWSI calculated by three models

IRT measurements and $VPD$ from 100/100 treatment in eleven sunny days after an irrigation event were used to establish a non-water stress baseline for maize in 2015. The canopy temperature, air temperature and $VPD$ at 11:00, 12:00, 13:00 and 14:00 h MST from each selected day were used to estimate the non-water stress baseline for Eq. (2) (Idso et al., 1981; Taghvaeian et al., 2014b). After determining the linear coefficients in Eq. (2), hourly CWSI-E was calculated based on Eqs. (1)–(3) at 11:00, 12:00, 13:00 and 14:00 h MST. Daily CWSI-E was obtained as an averaged CWSI-E value over these four hours.

The net radiation and air temperature at 11:00, 12:00, 13:00 and 14:00 h MST from each selected day, were used to calculate the seasonal average net radiation and temperature. Taken together with the slope and intercept of the non-water stress baseline (Eq. (2)), the seasonal average aerodynamic resistance and potential canopy resistance was calculated by Eqs. (8)–(9). A more detailed calculation procedure for other climate parameters (such as: $\gamma$, $\Delta$, and $c_p$) in CWSI-T1 and CWSI-T2 could be found in Allen et al. (1998).

Hourly CWSI at 11:00, 12:00, 13:00, and 14:00 h MST was calculated by three models from Jul 13 to Sept 20, 2015. Daily CWSI was then calculated by averaging the CWSI values over these four hours for each day.

#### 2.3.2. Water stress from sap flow measurement

Sap flow at 11:00, 12:00, 13:00, and 14:00 h MST in each day from Jul 28 to Sept 05, 2015 was used to calculate a stress index, $k_{s\_sap}$. Assuming the crop transpiration in 100/100 could represent the full transpiration condition, the measured crop water stress for deficit irrigation treatment was defined as:

$$k_{ssap} = 1 - Sap_i/Sap_1 \tag{10}$$

where: $Sap_1$ is the hourly sap flow measurement in 100/100 treatment in mm h$^{-1}$, and $Sap_i$ is the hourly measured transpiration in deficit treatment in mm h$^{-1}$.

### 2.4. Model comparison

The range of both $k_{s\_sap}$ and CWSI are analogous, such that CWSI = 0 indicates a well-watered crop, just as in a well-watered crop, $Sap_i = Sap_1$ thus $k_{s\_sap} = 0$ (Eq. (10)). Likewise, if transpiration is completely stopped (e.g. $Sap_i = 0$), then $k_{s\_sap} = 1$ and CWSI would also be maximized at 1. The differences between crop water stress estimated by the three models and sap flow measurements were evaluated by two statistical indicators, namely the mean bias difference (MBD) and the root mean square deviation (RMSD) (Nash and Sutcliffe, 1970; Willmott, 1982):

$$MBD = \frac{1}{n}\sum_{i}^{n} k_{s\,sap} - CWSI \tag{12}$$

$$RMSD = \sqrt{\frac{1}{n}\sum_{i}^{n} (k_{s\,sap} - CWSI)^2} \tag{13}$$

where: $k_{s\_sap}$ represents the water stress from sap flow measurement, CWSI is the crop water stress index, and n is the number of observations. All the calculations and statistical analysis have been done in *R* (Foundation for Statistical Computing, Vienna, Austria, and version 3.3.1).

## 3. Results

### 3.1. Parameters of non-water stress baseline for CWSI

Non-water stress baseline for maize in Greeley, CO in 2015 is shown in Fig. 2. Several baseline parameters obtained by previous studies for maize are listed in Table 3. The baseline in this study was similar to those obtained by previous studies in Greeley, CO. However, there are still some differences in the regression coefficients, especially for the intercept *a*, even when compared with the result obtained in the same field (DeJonge et al., 2015). In general, the slope *b* ranged from −2.0 to −1.8, while the intercept *a* ranged from 2.3 to 3.4, for maize in Greely, CO. This variation may have been caused by other factors such as wind speed, crop growth stages and IRT view angles, etc. Other studies have also reported changes in baseline parameters between years or between seasons. For example, Gonzalez-Dugo et al. (2014) reported that the intercept varied from 3.3 to 3.9 during a three-year experiment on citrus. When applying an empirical approach for irrigation management, the baseline was assumed unchanged for the same crop at a specific site. However, due to the observed variations in baseline parameters for maize in the same study area among years, it is necessary to investigate the uncertainty of CWSI caused by the variations of baseline parameters.

The seasonal average $\bar{r}_a$andd $\bar{r}_{cp}$ were 13.23 s m$^{-1}$ and 42.42 s m$^{-1}$, respectively. Jackson et al. (1981) stated that it was reasonable to use a constant $\bar{r}_a$, around 6–10 s m$^{-1}$. O'Toole and Real (1986) used the same method and obtained 14.9 s m$^{-1}$ and 56.3 s m$^{-1}$ for $\bar{r}_a$ and $\bar{r}_{cp}$, respectively. Tolk (1992) reported $\bar{r}_{cp}$ for corn was ranging from 30 ~ 110 s m$^{-1}$ during the growing season. Thus, the seasonal average $\bar{r}_a$ and $\bar{r}_{cp}$ obtained for CWSI-T2 in this study were reasonable.

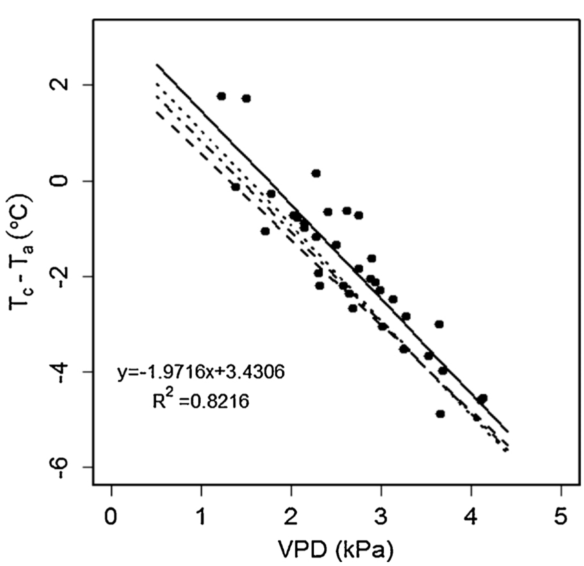


**Fig. 2.** Non-water stress baseline developed in this study ($(T_c - T_a)_l = b \times VPD + a$, where $T_c$ is canopy temperature, $T_a$ is air temperature, and *VPD* is vapor pressure deficit. Solid line and black dots), along with baselines development by DeJonge et al. (2015) (Segment Line), Taghvaeian et al. (2012) (), and Taghvaeian et al. (2014b) (Dotted Line) in Greeley, Colorado.

**Table 3**
Previous maize publications that report slope and intercept coefficients from fitted linear models, i.e., $(T_c - T_a)_l = b \times VPD + a$, where Tc is canopy temperature, Ta is air temperature, *VPD* is vapor pressure deficit, and *a* and *b* are coefficients.

| *b* | *a* | Location | Paper |
|---|---|---|---|
| −1.99 | 3.04 | Greeley, CO | Taghvaeian et al. (2014b) |
| −1.90 | 2.73 | Greeley, CO | Taghvaeian et al. (2012) |
| −1.97 | 3.11 | Tempe, Arizona | Idso et al. (1981) |
| −2.56 | 1.06 | Bushland, TEX | Yazar et al. (1999) |
| −1.93 | 0.84 | Carrington, ND | Stegman (1986) |
| −1.79 | 2.34 | Greeley, CO | DeJonge et al. (2015) |

### 3.2. Daily comparison of the calculated CWSI with sap flow measurement

Fig. 3 shows the daily CWSI values determined by three models and sap flow measurements for four irrigation treatments. In the case of 100/100, the well-watered crop, the values of CWSI-E and CWSI-T2 were relatively stable with a range of 0–0.2, while CWSI-T1 showed an increasing trend and was larger than 0.2 after Aug 20, 2015. In the case of deficit irrigation treatments (65/65, 40/40 and 40/80), CWSI-E and CWSI-T2 showed crop water stress in the vegetative stage, then gradually decreased when full irrigation was resumed in the reproductive stage, and then increased again when stress was applied in the maturation stage. CWSI-T1 underestimated the water stress in the vegetative stage, but showed water stress in both reproductive and maturation stage. CWSI-E and CWSI-T2 gave more reasonable water stress estimation, compared with CWSI-T1. The error bar in Fig. 3 was the standard deviation of eight replicates of sap flow measurements in each treatment.

The large standard deviation may be caused due to the following reasons. 1) Sap flow measurement itself has 5%–10% uncertainties (Green et al., 2003; Zhang et al., 2011). 2) Although the majority of soil texture in the experiment field is sandy and fine sandy loam, certain plots also include other soil textures such as Nunn clay loam and Otero sandy loam (Trout and Bausch, 2017). The difference in soil texture would lead to different response of crop to available soil water. However, the sap measurement is still able to show the variation of crop water stress during the growing season and among different irrigation treatments.

Examining stress indication over the entire measurement period, CWSI-T2 and CWSI-E gave better performance than CWSI-T1 (Table 4). CWSI-T2 and CWSI-E showed a close agreement with water stress measurement from sap flow in 40/40 and 40/80, and slightly overestimated crop water stress in 65/65 (negative MBD in Table 4, and Fig. 3). CWSI-T1 overestimated crop water stress in the reproductive and maturation stages, and extremely underestimated crop water stress in the vegetative stage for 40/40. Overall, crop water stress estimated by CWSI-T2 and CWSI-E showed a reasonable agreement with sap flow measurement, while CWSI-T1 failed to give reasonable estimation in the vegetative stage.

### 3.3. Growth stage comparison of three CWSI models

Crop water stress index by each model was also compared against water stress determined by sap flow measurements across the season in different growth stages (Table 5). In the vegetative stage, the values of CWSI-T1 were significantly underestimated as compared with the other

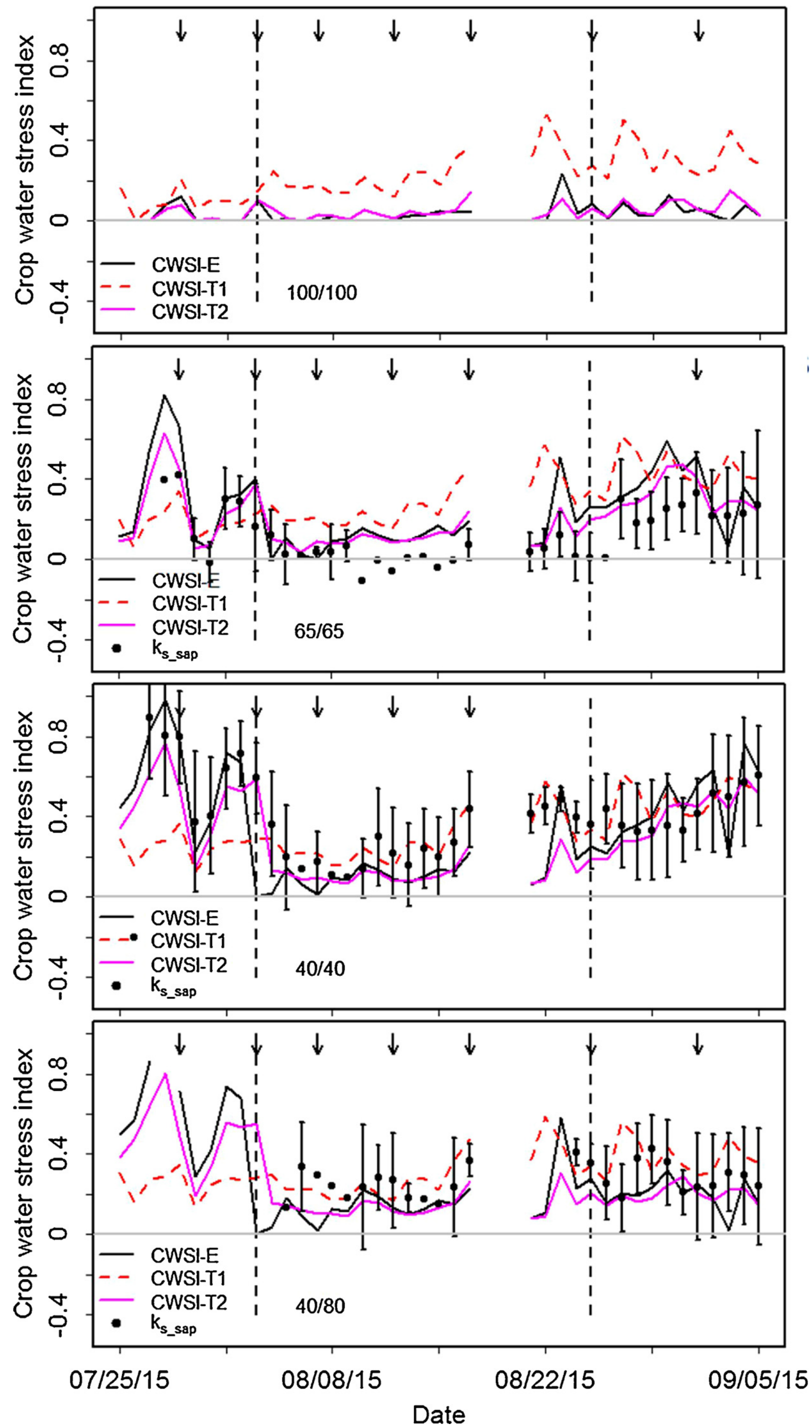


**Fig. 3.** Daily comparisons of three CWSI models with crop water stress determined by sap flow measurements ($k_{s\_sap}$). Error bars represent standard deviation of sap flow measurement. Vertical dashed lines denote transition between major growth stages (i.e., late vegetative, reproductive, and maturation, respectively). The black arrows on top indicate the irrigation events. The gap in the figure is due to the missing meteorological data in this period. No CWSI was calculated in this period.

methods, especially for 40/40 and 40/80 (both with 40% of ET). CWSI-T2 and CWSI-E reflected the increased water stress between treatments due to deficit irrigation in this period. When crops went into the reproductive stage, full irrigation was resumed and $k_{s\_sap}$ values ranged 0–0.19. The values of CWSI-T2 and CWSI-E in this period decreased compared to the values in the vegetative stage and closed to the $k_{s\_sap}$ values; however, the values of CWSI-T1 showed a slight increase and were larger than 0.2. When crops reached the maturation stage, the deficit irrigation was resumed in the 65/65 and 40/40, while the 100/100 and 40/80 received full and nearly-full irrigation, respectively. Thus, CWSIs from all three models and sap flow were increased in 65/65 and 40/40; and the values of CWSI-E and CWSI-T2 did not change in 100/100 and 80/80 due to similar water conditions in the reproductive stage. The values of CWSI-T1 in 100/100 increased, which is against the observed seasonal crop water stress trend from sap flow measurement and irrigation management. The values of CWSI-E and CWSI-T2 in 40/80 in the maturation stage were lower than those in the vegetative stage, which is consistent with the observed crop water stress trend from sap flow measurement and irrigation management. Again, the value of CWSI-T1 in 40/80 in the maturation stage was even higher than the value in the vegetative period, and the value of CWSI-T1 shown an increasing trend from vegetative to maturation stage in all treatments, which indicated that

**Table 4**
Seasonal error estimates for crop water stress index by three CWSI models as compared against transpiration declines determined from sap flow measurements ($k_{s\_sap}$). Veg – Vegetative growth stage. Rep – Reproductive growth stage. Mat – Maturation growth stage. MBD – mean bias difference. RMSD – root mean square deviation. N/A-Data not available (no sap flow measurement of 40/80 in the vegetative period). Treatment designations are as described in Table 1.

| Growth Stage | Model | 65/65 | | 40/40 | | 40/80 | | All Treatment | |
|---|---|---|---|---|---|---|---|---|---|
| | | MBD | RMSD | MBD | RMSD | MBD | RMSD | MBD | RMSD |
| Veg | CWSI-E | −0.13 | 0.21 | 0.01 | 0.10 | N/A | N/A | −0.06 | 0.16 |
| | CWSI-T1 | 0.02 | 0.11 | 0.37 | 0.39 | N/A | N/A | 0.21 | 0.30 |
| | CWSI-T2 | −0.09 | 0.14 | 0.10 | 0.14 | N/A | N/A | 0.01 | 0.14 |
| Rep | CWSI-E | −0.11 | 0.16 | 0.16 | 0.22 | 0.10 | 0.13 | 0.05 | 0.18 |
| | CWSI-T1 | −0.28 | 0.30 | −0.03 | 0.11 | −0.03 | 0.10 | −0.12 | 0.20 |
| | CWSI-T2 | −0.14 | 0.16 | 0.11 | 0.16 | 0.07 | 0.10 | 0.01 | 0.15 |
| Mat | CWSI-E | −0.14 | 0.19 | −0.02 | 0.16 | 0.09 | 0.12 | −0.02 | 0.16 |
| | CWSI-T1 | −0.26 | 0.28 | −0.08 | 0.15 | −0.12 | 0.17 | −0.15 | 0.20 |
| | CWSI-T2 | −0.15 | 0.18 | −0.02 | 0.11 | 0.04 | 0.09 | −0.04 | 0.13 |

**Table 5**
Crop stress across the season as indicated by three CWSI models and transpiration declines determined from sap flow measurements ($k_{s\_sap}$). Values are averaged over each growth stage. Veg – Vegetative growth stage. Rep – Reproductive growth stage. Mat – Maturation growth stage. N/A-Data not available.

| Growth Stage | Model | 100/100 | 65/65 | 40/40 | 40/80 |
|---|---|---|---|---|---|
| Veg | CWSI-E | 0.03 | 0.40 | 0.66 | 0.62 |
| | CWSI-T1 | 0.13 | 0.23 | 0.30 | 0.30 |
| | CWSI-T2 | 0.05 | 0.35 | 0.56 | 0.57 |
| | $k_{s\_sap}$ | N/A | 0.25 | 0.66 | N/A |
| Rep | CWSI-E | 0.04 | 0.15 | 0.13 | 0.16 |
| | CWSI-T1 | 0.27 | 0.31 | 0.32 | 0.33 |
| | CWSI-T2 | 0.08 | 0.18 | 0.17 | 0.19 |
| | $k_{s\_sap}$ | N/A | 0.03 | 0.29 | 0.26 |
| Mat | CWSI-E | 0.05 | 0.35 | 0.46 | 0.20 |
| | CWSI-T1 | 0.35 | 0.47 | 0.52 | 0.42 |
| | CWSI-T2 | 0.10 | 0.37 | 0.46 | 0.25 |
| | $k_{s\_sap}$ | N/A | 0.22 | 0.43 | 0.28 |

CWSI-T1 did not respond to stress throughout the growing season. Thus, only CWSI-E and CWSI-T2 well described crop water stress difference between treatments and growth stages.

### 3.4. Relationship between the averaged crop water stress indexes and yield

All CWSIs show significantly negative trends with the yield (Fig. 4). All CWSIs well reflected the decreasing of yield caused by increasing of crop water stress. However, the yield decreasing trend (slope) of each yield-CWSI linear relationship is quite different. The slopes of CWSI-E and CWSI-T2 are similar and close to the slope of $k_{s\_sap}$, while the slope of CWSI-T1 is the highest and differs from $k_{s\_sap}$. The high slope of CWSI-T1 is mainly due to the overestimation of crop water stress in the maturation period for 100/100 and 40/80 (Table 5 and Fig. 4). Thus, CWSI-E and CWSI-T2 could better describe the decreasing of yield caused by water stress than CWSI-T1.

### 3.5. Uncertainty of CWSI-E and CWSI-T2

CWSI difference of CWSI-E model caused by the different parameters of the non-stressed baseline is shown in Fig. 5A and B. The intercept and slope parameters, $a$ and $b$, are within the ranges reported in the literature (Table 3, Fig. 2). Compared to intercept $a$, the uncertainty range of slope $b$ was small for maize in Greeley, CO, so the impact of slope $b$ on CWSI was also quite small. Furthermore, intercept $a$ appeared to have a greater effect on CWSI than did slope $b$ per magnitude change (i.e., $\Delta a = \pm 0.2$ vs $\Delta b = \pm 0.2$). Gonzalez-Dugo et al. (2014) also reported similar slope coefficients, but large differences in intercept coefficients across years over a three-year experiment. Thus, it is important to define intercept $a$ carefully for CWSI-E model.

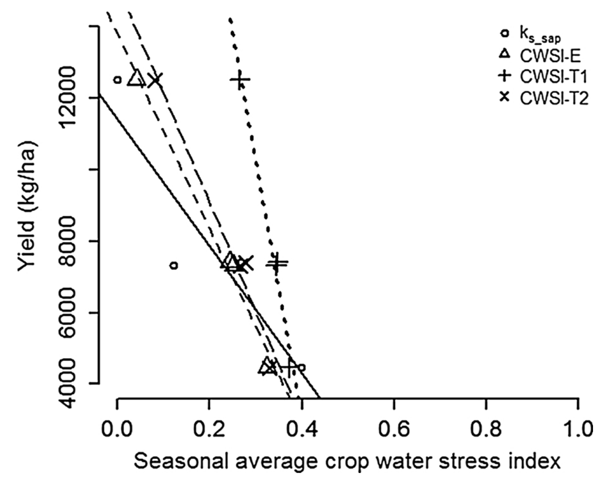


**Fig. 4.** Relationships between the seasonal averaged CWSIs and yield (The dot line- CWSI-T1; long dash line – CWSI-T2; short dash line – CWSI-E; black line – $k_{s\_sap}$). $k_{s\_sap}$ for 100/100 treatment supposed to be 0.

Similarly, CWSI difference from CWSI-T2 decreased with increasing VPD and intercept $a$ also had more influence on CWSI than slope $b$ did (Fig. 5C–D). Moreover, CWSI difference from CWSI-T2 model was smaller than CWSI-E, when given same parameter changes.

## 4. Discussion

### 4.1. CWSI-T1 vs. CWSI-T2

From daily and seasonal analysis of CWSI-T1, we found that CWSI-T1 showed the water stress difference between treatments, and was also relative stable due to the inclusion of additional climate factors in its calculation (Figs. 3–4 and Table 4). This result is well-supported by previous research (Ben-Gal et al., 2009; Horst et al., 1989; Yuan et al., 2004). However, the comparison to sap flow data revealed that CWSI-T1 underestimated crop water stress for deficit-irrigated maize during the vegetative period (Table 4). Agam et al. (2013) also reported that the underestimation of crop water stress for full irrigated olive trees by CWSI-T1. Crop water stress estimated by CWSI-T1 showed an increasing trend for all treatments (Table 4), and failed to adequately respond to irrigation events and describe water stress difference between growth stages (Fig. 3, Tables 4 and 5). Previous research suggests that the uncertainty of the aerodynamic resistance may influence the result of CWSI-T1, but the mechanism is still unknown (Agam et al., 2013; Barbosa da Silva and Ramana Rao, 2005; Stockle and Dugas, 1992).

We observed that with increasing crop height, the aerodynamic resistance decreased (Fig. 6A). The consequence of this decrease in aerodynamic resistance resulted in a smaller upper limit of $T_c$-$T_a$ (Eq. 5). The

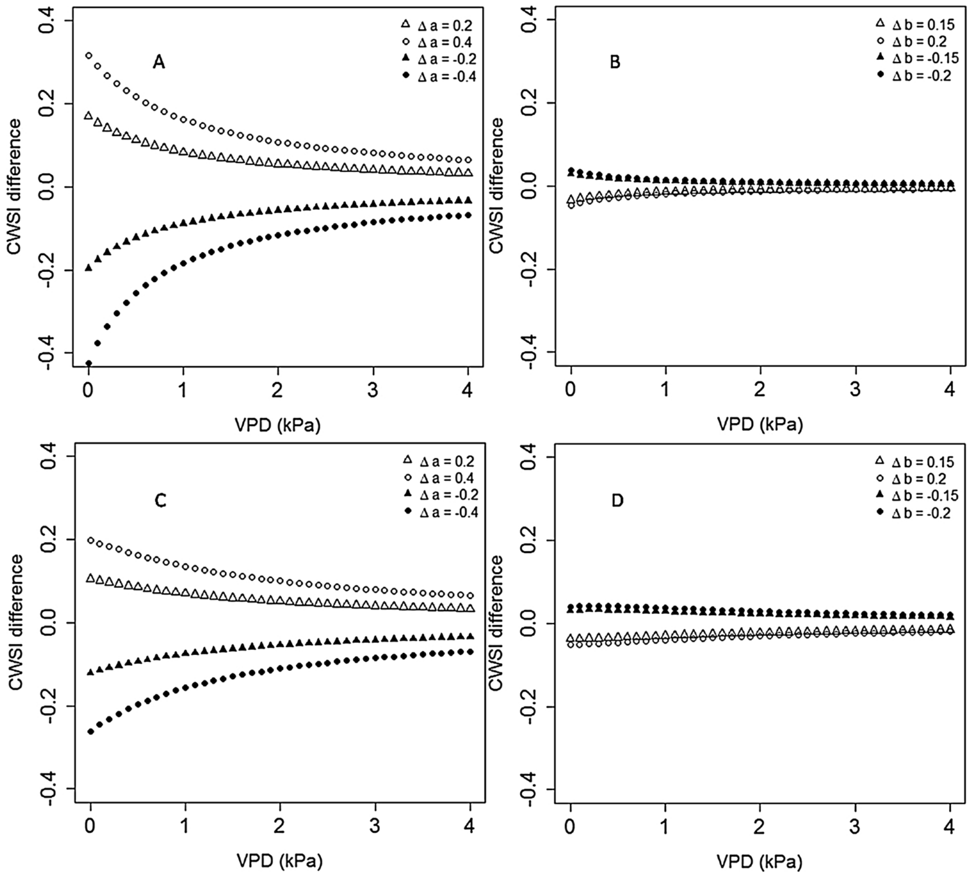


**Fig. 5.** CWSI difference of CWSI-E model with changing of parameters $a$ (A) and $b$ (B) of the non-stress baseline, and CWSI difference of CWSI-T2 model with changing of parameters a (C) and $b$ (D), ($b = -1.85$, $a = 2.9$, $T_c - T_a = 3.4\,^{\circ}\mathrm{C}$).

difference between the upper and lower limits of CWSI-T1 also decreased, so the estimated crop water stress exhibited an increasing trend (Eq. (1)). From Fig. 6B, we also noticed the large difference between the upper and lower limits of CWSI-T1 in the vegetative period, which is why crop water stress for 40/40 and 40/80 were underestimated during this period.

Correct estimation of aerodynamic resistance is critical to provide a reasonable assessment of crop water stress using the CWSI-T1 method, which would require accurate measurements (crop height, wind speed, air temperature, etc.) (Tolk et al., 1995). CWSI-T2 method can be a good alternative to CWSI-T1, because it was better aligned with water stress estimates from sap flow and well described water stress between treatments and growth stages. At the same time, CWSI-T2 and CWSI-E could better describe the yield reduction due to crop water stress. In a practical view, the use of a seasonal constant for the aerodynamic resistance parameter is acceptable for theoretical approaches (Clawson et al., 1989; Jalali-Farahani et al., 1993).

### 4.2. CWSI-E vs. CWSI-T2

Although the results indicated that the CWSI-E model was closely aligned with $k_{s\_}sap$, the limitation of the CWSI-E method is quite significant. In the uncertainty study (Section 3.5), we assumed the parameters for CWSI-E and CWSI-T2 were not changed except for $a$, $b$ and $VPD$. It supposed to be an efficient way to examine the sensitivity of model parameters and uncertainty of the model. CWSI-E was more sensitive to the change of baseline parameter than CWSI-T2 was. The reason for this

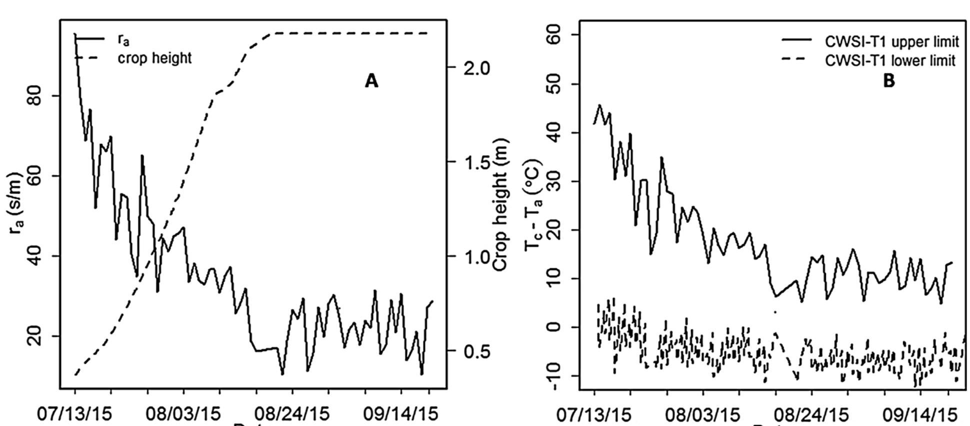


**Fig. 6.** Relationships between aerodynamic resistance ($r_a$) and crop height (A); Upper and lower boundary of $T_c - T_a$ in CWSI-T1 model (B).

may be that CWSI-T2 model incorporates more climate factors. The large uncertainty caused by changing parameter $a$ and $b$ in low VPD region (Fig. 5) may indicate that both CWSI-T2 and CWSI-E should not be applied under low VPD condition, as reported by Stockle and Dugas (1992).

In addition to the uncertainty in CWSI caused by small changes in the non-stressed baseline coefficients (Fig. 5), changing climate factors (such as: $R_n$, $\Delta$, $r_a$, $r_c$ and $c_p$) are also associated with significant variation in CWSI-E (Stockle and Dugas, 1992). Theoretically the influence of these climate factors on CWSI-E could be determined by comparing it with the output from CWSI-T2 model. Although these two models share the same non-water stress baseline, CWSI-T2 took these climate variables into account. The difference between CWSI-E and CWSI-T2 was quite small for 100/100, which experienced minimal water stress. Nevertheless, CWSI-E showed some fluctuations under deficit irrigation and large differences between CWSI-E and CWSI-T2 were found in some days, e.g., Aug 23. CWSI-E also yielded CWSI values larger than 1 on July 28 for 40/80. Although the uncertainties remain by using seasonal estimates of $r_a$ and $r_{cp}$ determined from non-water stress baseline, incorporating climate factors in the calculation of the upper and lower boundary limits (i.e., CWSI-T2) are likely to improve the stability of water stress estimation (Clawson et al., 1989; Jalali-Farahani et al., 1993). CWSI-T2 was also more closely aligned with $k_{s\_sap}$ than CWSI-E in all four treatments, and thus, we recommend CWSI-T2 over CWSI-E model.

## 5. Conclusions

Considering the uncertainty of crop stress determined from sap flow measurement, CWSI-E and CWSI-T2 models gave reasonable water stress estimates. However, crop water stress from CWSI-T1 exhibited a constant increasing trend through growing season and did not adequately predict changes in crop water status resulting from neither irrigation events nor growth stage differences. We therefore suggest that CWSI-T1 may not be a reliable method for determining stress in maize, although CWSI-T1 could reflect the crop water status between treatments.

Assuming a seasonal average aerodynamic resistance, the CWSI-T2 model performed better than the empirical method. Both CWSI-T2 and CWSI-E could well predict crop water stress between irrigation events as well as across growth stages. By including the climate factors, crop water stress estimated from CWSI-T2 exhibited better alignment with sap flow than did CWSI-E.

The uncertainty of both CWSI-T2 and CWSI-E decreased with the increasing of VPD and the intercept of non-water stress baseline was the main source of error. The uncertainty from CWSI-T2 was less than that from CWSI-E. We recommend CWSI-T2 model for assessing crop water stress, although it requires more climate data.

## Acknowledgements

The authors would like to thank the technical staff who assisted with data collection and management, particularly Liam Cummins for managing IRTs, and Jason Young for managing sap flow.

## Appendix A

Table A1

**Table A1**
Symbol and abbreviation list.

| Symbol | Description | Unit |
|---|---|---|
| $a$ | Intercept of linear regression parameters of $(T_c - T_a)_l$ on air vapor pressure deficit ($VPD$) | – |
| $b$ | Intercept of linear regression parameters of $(T_c - T_a)_l$ on air vapor pressure deficit ($VPD$) | – |
| $c_p$ | Heat capacity of air | J kg$^{-1}$ °C |
| CWSI-E | Crop water stress index from an empirical method | – |
| CWSI-T1 | Crop water stress index from theoretical method | – |
| CWSI-T2 | Crop water stress index from theoretical method with seasonal average aerodynamic resistance | – |
| $d$ | Displacement height | m |
| $\bar{\Delta}$ | Seasonal average slope of saturated vapor pressure- temperature relationship | Pa °C$^{-1}$ |
| $\Delta$ | Change (slope) of saturation vapor pressure with temperature | Pa °C$^{-1}$ |
| $e$ | Air vapor pressure | Pa |
| $e*$ | Air saturated vapor pressure at $T_c$ | |
| $G$ | Heat flux consumed by soil | J m$^{-2}$ s$^{-1}$ |
| $\gamma$ | Psychrometric constant | Pa °C$^{-1}$ |
| $h$ | Height of crop | m |
| $\bar{k}_{s\_sap}$ | Measured crop water stress from sap flow | – |
| $R_n$ | Net radiation | J m$^{-2}$ s$^{-1}$ |
| $r_a$ | Aerodynamic resistance | s m$^{-1}$ |
| $r_c$ | Canopy resistance | s m$^{-1}$ |
| $r_{cp}$ | Canopy resistance under full transpiration condition | s m$^{-1}$ |
| $\bar{R}_{\mathrm{n}}$ | Seasonal average net radiation | J m$^{-2}$ s$^{-1}$ |
| $\bar{r}_{\mathrm{cp}}$ | Seasonal average canopy resistance under full transpiration condition | s m$^{-1}$ |
| $\bar{r}_{\mathrm{a}}$ | Seasonal average Aerodynamic resistance | s m$^{-1}$ |
| $Sap_1$ | Sap flow measurement in full irrigated treatment | mm h$^{-1}$ |
| $Sap_i$ | Sap flow measurement in deficit irrigation treatment $i$ | mm h$^{-1}$ |
| $T_c$ | Canopy temperature | °C |
| $T_a$ | Air temperature | °C |
| $(T_c - T_a)_u$ | Upper boundary of temperature difference between air and canopy | °C |
| $(T_c - T_a)_l$ | Lower boundary of temperature difference between air and canopy | °C |
| $u$ | Wind speed at height $z$ | m s$^{-1}$ |
| $VPD$ | Air vapor pressure deficit | Pa |
| $VPG$ | Difference between the saturation vapor pressure evaluated at air temperature ($T_a$) and at a higher air temperature equal to air temperature plus $a$ | Pa |
| $z_o$ | Roughness length | m |
| $z$ | Reference height | m |

## References


Agam, N., Cohen, Y., Berni, J., Alchanatis, V., Kool, D., Dag, A., Yermiyahu, U., Ben-Gal, A., 2013. An insight to the performance of crop water stress index for olive trees. Agric. Water Manage. 118, 79–86.

Allen, R.G., Pereira, L.S., Raes, D., Smith, M., 1998. Crop Evapotranspiration-Guidelines for Computing Crop Water Requirements-FAO Irrigation and Drainage Paper 56 300. pp. D05109.

Ballester, C., Jiménez-Bello, M.A., Castel, J.R., Intrigliolo, D.S., 2013. Usefulness of thermography for plant water stress detection in citrus and persimmon trees. Agric. For. Meteorol. 168, 120–129.

Barbosa da Silva, B., Ramana Rao, T.V., 2005. The CWSI variations of a cotton crop in a semi-arid region of Northeast Brazil. J. Arid Environ. 62, 649–659.

Ben-Gal, A., Agam, N., Alchanatis, V., Cohen, Y., Yermiyahu, U., Zipori, I., Presnov, E., Sprintsin, M., Dag, A., 2009. Evaluating water stress in irrigated olives: correlation of soil water status, tree water status, and thermal imagery. Irrig. Sci. 27, 367–376.

Cammalleri, C., Rallo, G., Agnese, C., Ciraolo, G., Minacapilli, M., Provenzano, G., 2013. Combined use of eddy covariance and sap flow techniques for partition of ET fluxes and water stress assessment in an irrigated olive orchard. Agric. Water Manage. 120, 89–97.

Chabot, R., Bouarfa, S., Zimmer, D., Chaumont, C., Duprez, C., 2002. Sugarcane transpiration with shallow water-table: sap flow measurements and modelling. Agric. Water Manage. 54, 17–36.

Chalmers, D.J., Mitchell, P.D., Van Heek, L., 1981. Control of peach tree growth and productivity by regulated water supply, tree density, and summer pruning [Trickle irrigation]. J. Am. Soc. Hortic. Sci. (U. S. A.) 106, 307–312.

Clawson, K., Jackson, R., Pinter, P., 1989. Evaluating plant water stress with canopy temperature differences. Agron. J. 81, 858–863.

Colaizzi, P.D., O'Shaughnessy, S., Evett, S., Howell, T.A., 2012. Using plant canopy temperature to improve irrigated crop management. In: Proceedings of the 24th Annual Central Plains Irrigation Conference. Colby KS.

DeJonge, K.C., Taghvaeian, S., Trout, T.J., Comas, L.H., 2015. Comparison of canopy temperature-based water stress indices for maize. Agric. Water Manage. 156, 51–62.

Emekli, Y., Bastug, R., Buyuktas, D., Emekli, N.Y., 2007. Evaluation of a crop water stress index for irrigation scheduling of bermudagrass. Agric. Water Manage. 90, 205–212.

Geerts, S., Raes, D., 2009. Deficit irrigation as an on-farm strategy to maximize crop water productivity in dry areas. Agric. Water Manage. 96, 1275–1284.

Gonzalez-Dugo, V., Zarco-Tejada, P.J., Fereres, E., 2014. Applicability and limitations of using the crop water stress index as an indicator of water deficits in citrus orchards. Agric. For. Meteorol. 198-199, 94–104.

Green, S., Clothier, B., Jardine, B., 2003. Theory and practical application of heat pulse to measure sap flow. Agron. J. 95, 1371–1379.

Horst, G., O'toole, J., Faver, K., 1989. Seasonal and species variation in baseline functions for determining crop water stress indices in turfgrass. Crop science 29, 1227–1232.

Idso, S.B., Jackson, R.D., Pinter, P.J., Reginato, R.J., Hatfield, J.L., 1981. Normalizing the stress-degree-day parameter for environmental variability. Agric. Meteorol. 24, 45–55.

Jackson, R.D., Idso, S.B., Reginato, R.J., Pinter, P.J., 1981. Canopy temperature as a crop water stress indicator. Water Resour. Res. 17, 1133–1138.

Jackson, R.D., Kustas, W.P., Choudhury, B.J., 1988. A reexamination of the crop water stress index. Irrig. Sci. 9, 309–317.

Jalali-Farahani, H., Slack, D.C., Kopec, D.M., Matthias, A.D., 1993. Crop water stress index models for Bermudagrass turf: a comparison. Agron. J. 85, 1210–1217.

Jara, J., Stockle, C.O., 1999. Simulation of water uptake in maize, using different levels of process detail. Agron. J. 91.

Jensen, M.E., Allen, R.G., 2016. Evaporation, Evapotranspiration, and Irrigation Water Requirements. American Society of Civil Engineers, Reston, VA.

Nash, J.E., Sutcliffe, J.V., 1970. River flow forecasting through conceptual models part I—A discussion of principles. J. Hydrol. 10, 282–290.

Nielsen, D., 1990. Scheduling irrigations for soybeans with the crop water stress index (CWSI). Field Crops Res. 23, 103–116.

O'Shaughnessy, S.A., Evett, S.R., Colaizzi, P.D., Howell, T.A., 2010. Automatic irrigation scheduling of grain sorghum using a CWSI and time threshold. In: 5th National Decennial Irrigation Conference Proceedings. 5–8 December 2010, Phoenix Convention Center, Phoenix, Arizona USA. American Society of Agricultural and Biological Engineers p. 1.

O'Toole, J., Real, J., 1986. Estimation of aerodynamic and crop resistances from canopy temperature. Agron. J. 78, 305–310.

Payero, J.O., Irmak, S., 2006. Variable upper and lower crop water stress index baselines for corn and soybean. Irrig. Sci. 25, 21–32.

Sakuratani, T., 1981. A heat balance method for measuring water flux in the stem of intact plants. J. Agric. Meteorol. 31, 9–17.

Stegman, E.C., 1986. Efficient irrigation timing methods for corn production. Trans ASAE 29 (1), 203–210.

Stockle, C.O., Dugas, W.A., 1992. Evaluating canopy temperature-based indices for irrigation scheduling. Irrigation Science 13, 31–37.

Taghvaeian, S., Chávez, J.L., Hansen, N.C., 2012. Infrared thermometry to estimate crop water stress index and water use of irrigated maize in Northeastern Colorado. Remote Sens. 4, 3619–3637.

Taghvaeian, S., Comas, L., DeJonge, K.C., Trout, T.J., 2014a. Conventional and simplified canopy temperature indices predict water stress in sunflower. Agric. Water Manage. 144, 69–80.

Taghvaeian, S., Chávez, J.L., Bausch, W.C., DeJonge, K.C., Trout, T.J., 2014b. Minimizing instrumentation requirement for estimating crop water stress index and transpiration of maize. Irrig. Sci. 32 (1), 53–65.

Tolk, J.A., Howell, T.A., Steiner, J.L., Krieg, D.R., 1995. Aerodynamic characteristics of corn as determined by energy balance techniques. Agron. J. 87, 464–473.

Tolk, J.A., 1992. Corn Aerodynamic and Canopy Surface Resistances and Their Role in Sprinkler Irrigation Efficiency. Texas Tech University.

Trout, T.J., Bausch, W.C., 2017. USDA-ARS Colorado maize water productivity data set. Irrig. Sci. 35, 241–249.

Wang, L., Qiu, G.Y., Zhang, X., Chen, S., 2005. Application of a new method to evaluate crop water stress index. Irrig. Sci. 24, 49–54.

Willmott, C.J., 1982. Some comments on the evaluation of model performance. Bull. Am. Meteorol. Soc. 63, 1309–1313.

Yazar, A., Howell, T., Dusek, D., Copeland, K., 1999. Evaluation of crop water stress index for LEPA irrigated corn. Irrig. Sci. 18, 171–180.

Yuan, G., Luo, Y., Sun, X., Tang, D., 2004. Evaluation of a crop water stress index for detecting water stress in winter wheat in the North China Plain. Agric. Water Manage. 64, 29–40.

Zhang, Y., Kang, S., Ward, E.J., Ding, R., Zhang, X., Zheng, R., 2011. Evapotranspiration components determined by sap flow and microlysimetry techniques of a vineyard in northwest China: dynamics and influential factors. Agric. Water Manage. 98, 1207–1214.

Zhao, P., Li, S., Li, F., Du, T., Tong, L., Kang, S., 2015. Comparison of dual crop coefficient method and Shuttleworth–Wallace model in evapotranspiration partitioning in a vineyard of northwest China. Agric. Water Manage. 160, 41–56.